NASA Contractor Report 2949

Mean Velocity, Turbulence Intensity and Turbulence Convection Velocity Measurements for a Convergent Nozzle in a Free Jet Wind Tunnel

C. J. McColgan and R. S. Larson

CONTRACT NAS3-17866
APRIL 1978

NASA

NASA Contractor Report 2949

Mean Velocity, Turbulence Intensity and Turbulence Convection Velocity Measurements for a Convergent Nozzle in a Free Jet Wind Tunnel

C. J. McColgan and R. S. Larson
Pratt & Whitney Aircraft Group
United Technologies Corporation
East Hartford, Connecticut

Prepared for
Lewis Research Center
under Contract NAS3-17866

National Aeronautics
and Space Administration

**Scientific and Technical
Information Office**

1978

TABLE OF CONTENTS

	Page No.
1.0 SUMMARY	1
2.0 INTRODUCTION	2
2.1 Background	2
2.2 Investigation Description	2
3.0 EXPERIMENTAL DESCRIPTION	4
3.1 Test Apparatus	4
3.1.1 UTRC Facility	4
3.1.2 Hot Wire Apparatus	4
3.2 Data Acquisition	7
3.3 Test Definition	9
3.3.1 Mean Velocity, Turbulence Velocity and Turbulence Spectra	9
3.3.2 Cross Correlation Coefficients and Convection Velocities	9
3.4 Test Procedure	10
3.4.1 Determination of Model Nozzle and Wind Tunnel Velocities	10
3.4.2 Anemometer Calibration	11
4.0 RESULTS AND DISCUSSION	13
4.1 Mean Velocity	13
4.2 Mixing Layer Growth	13
4.3 Turbulence Measurements	15
4.3.1 Turbulence Spectra	15
4.3.2 Turbulence Intensity	16
4.4 Turbulence Convection Velocity	18
5.0 SUMMARY	21
APPENDIX A ANALYSIS OF ERRORS	22
APPENDIX B TABULATION OF CONVECTION VELOCITIES	23

1.0 SUMMARY

The effects of flight on the mean flow and turbulence properties of a jet in a flight environment were determined for a 0.056 m (2.22 in.) circular jet in a free jet wind tunnel. The nozzle exit velocity was 122 m/sec (400 ft/sec), and the wind tunnel velocity was set at 0, 12.2, 36.6, and 61.0 m/sec (0, 40, 120, and 200 ft/sec). Measurements of flow properties including mean velocity, turbulence intensity and spectra, and eddy convection velocity were carried out using two linearized hot wire anemometers. Normalization factors were determined for the mean velocity and turbulence convection velocity.

2.0 INTRODUCTION

2.1 BACKGROUND

Extensive use of noise absorbing materials in the inlet and exhaust ducting of modern high bypass ratio turbofan engines has reduced the noise radiated by fans, compressors, turbines and burners to the level that the jet noise (noise generated in the exhaust plume by mixing the high velocity jet with the ambient air) is an important part of the total noise signature of current aircraft. The characteristics of jet noise from turbojet and turbofan engines have been well documented under static conditions. However, aircraft noise certification limits must be satisfied under actual aircraft flyover conditions during take-off and approach operations. Thus, it is important that methods be developed to more accurately predict the jet noise under flight conditions.

The effect of flight on the jet noise of a circular jet exhaust has been simulated by testing in wind tunnels. (Refs. 1, 2) Noise measurements obtained in wind tunnel tests show that the jet exhaust noise of nozzles operating subsonically is reduced by forward velocity from the static levels at all measurement angles. However, noise measurements obtained from some aircraft flyover tests (Ref. 3) have shown less noise reduction than indicated by the results of the wind tunnel tests. In order to help resolve the differences in wind tunnel and flyover results, it is necessary to understand the effects of flight on the fundamental mechanisms of jet noise generation. Measurement was made of changes caused by flight on the basic aerodynamic parameters responsible for noise generation to provide a more basic understanding of the effect of flight on jet noise than was previously available. This work was accomplished under NASA Contract NAS3-17866.

The turbulence characteristics of an axisymmetric jet in a static environment have been thoroughly investigated (Refs. 4, 5, 6). The corresponding data for a jet in a flight environment are less comprehensive. In References 7, 8, and 9, the turbulence properties of a plane, two dimensional mixing layer were measured. However, such a mixing layer may not simulate the shear layer of an axisymmetric jet in a flight environment. The mean velocity and turbulence for an axisymmetric jet in a flight environment were determined in Reference 10, but the other important turbulence properties affecting jet noise, such as turbulence convection velocity, were not measured. An extensive set of data was obtained in Reference 11 for a coannular nozzle with an area ratio (secondary to primary) of 10, but for a low area ratio coannular nozzle, the structure of the inner shear layer would be affected by the developing outer shear layer at large downstream positions. Therefore, a consistent set of data for the basic aerodynamic properties, such as mean velocity, turbulence intensity, and turbulence convection velocity, for a jet in a flight environment was unavailable prior to the tests reported herein.

2.2 INVESTIGATION DESCRIPTION

The current investigation consisted of the measurement of the mean velocity, turbulence intensity, and turbulence convection velocity of a 0.056 m (2.22 in.) diameter jet in a free jet wind tunnel with a diameter of 0.91 m (36 in.). These measurements can provide the basis of an investigation of the effects of flight on jet noise (Ref. 12). The jet velocity was held constant at 122 m/sec (400 ft/sec), and the wind tunnel velocity was set at 0, 12.2, 36.6,

and 61.0 m/sec (0, 40, 120, and 200 ft/sec). Detailed measurements were taken at two axial stations for the static jet and three axial stations for wind tunnel velocities of 12.2, 36.6, and 61.0 m/sec (40, 120, and 200 ft/sec). The temperatures of the jet and wind tunnel were the ambient air temperature. At each axial station mean velocity and turbulence intensity profiles were obtained, and convection velocities were determined at three radial stations in the jet shear layer per axial station.

The apparatus and procedure used to obtain the aerodynamic data is described in Section 3.0. The mean flow and turbulence properties measured were correlated with jet wind tunnel relative velocity and are discussed in Section 4.0. Section 5.0 contains a summary of the fundamental results of this study. All the basic data obtained are published in companion report NASA CR-135238.

3.0 EXPERIMENTAL DESCRIPTION

3.1 TEST APPARATUS

3.1.1 UTRC Facility

The investigation was carried out in the United Technologies Research Center Acoustic Research Tunnel (Ref. 13), a free jet wind tunnel which provides an anechoic environment for flight simulation of aircraft and jet engine noise sources. Figure 1 is a schematic of the tunnel configuration, and Figure 2 shows the layout of the test chamber including far field microphones and air heaters not used in this experiment. The blower and drive motor for the tunnel flow were downstream of the test section while the model nozzle flow was provided by compressors. Adjustable louvers provided control of the tunnel velocity. Honeycomb and screens were located in the inlet and, in conjunction with a contraction ratio of 11.5, provided a uniform low turbulence test section flow.

The nozzle employed for these measurements was a 0.056 m (2.22 in.) diameter coaxial nozzle with an internal splitter (see Figure 3). Since the UTRC facility was being used to test coannular nozzles, a splitter was required to provide a uniform aerodynamic flow between the primary and secondary streams which were supplied at the same conditions. Normally, independent air controls are used to supply the fan and primary nozzles, but a bypass allowing both streams to operate from the same air supply was used for this test. A more uniform initial velocity profile was achieved in this manner. The ratio of the tunnel to nozzle exit diameter was 16, resulting in an area ratio of 208 which was sufficient to insure that the tunnel shear layer did not affect the jet flow.

3.1.2 Hot Wire Apparatus

A single hot wire probe was used to measure mean velocity and turbulence intensity profiles, and its signal was analyzed to provide frequency spectra and autocorrelations for selected points in the shear layer. The signals from two hot wire probes, mounted on traverse mechanisms, were cross correlated for varying values of probe separation. Normalized cross correlations and axial convection velocities were determined from the cross correlation records. The upstream probe, denoted as probe "A", traversed radially, while the downstream probe, denoted as probe "B", traversed axially along the jet.

Thermo-Systems, Inc., Model 1210-T1.5, standard hot wire probes were used in conjunction with Model 1054A anemometers for the data acquisition. The sensors were 1.3 mm long and 0.004 mm in diameter, and the probes were operated in the constant temperature mode. The anemometer bridge outputs were linearized to simplify data analysis. The signals from both probes were band-pass filtered from 0-20 kHz with Krohn-Hite filters to remove a spurious electrical resonance in the frequency range of 200 to 500 kHz. This oscillation seemed to be sensor dependent, in that changing the wire would sometimes reduce or eliminate the resonance. Several sensors were tried, and the ones which had the best frequency response and minimum resonance were used for the measurements. At 20 kHz the spectrum levels were 30 dB lower than the levels at the spectrum peak frequency which was sufficient to insure that filtering did not affect the results of this study. Figure 4 shows the hot wire probes, probe holders, and traverse mechanisms.

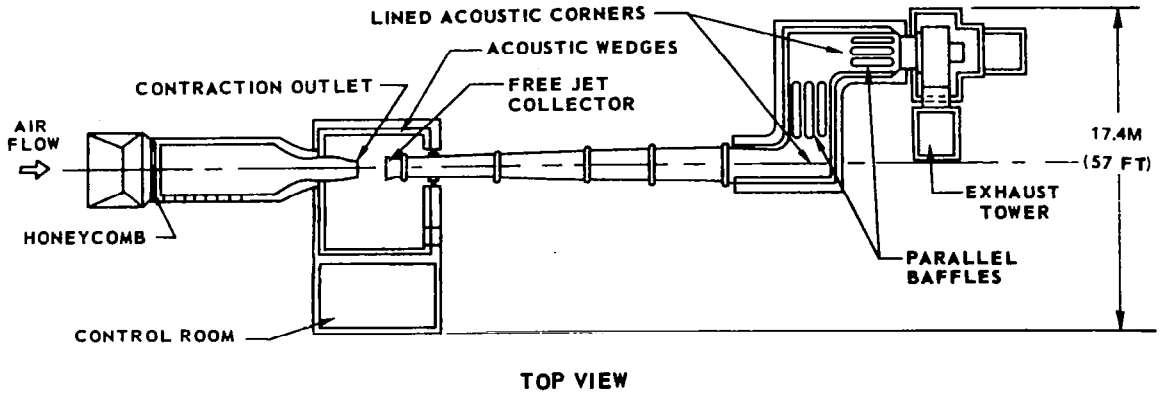

Figure 1 UTRC Acoustic Research Facility

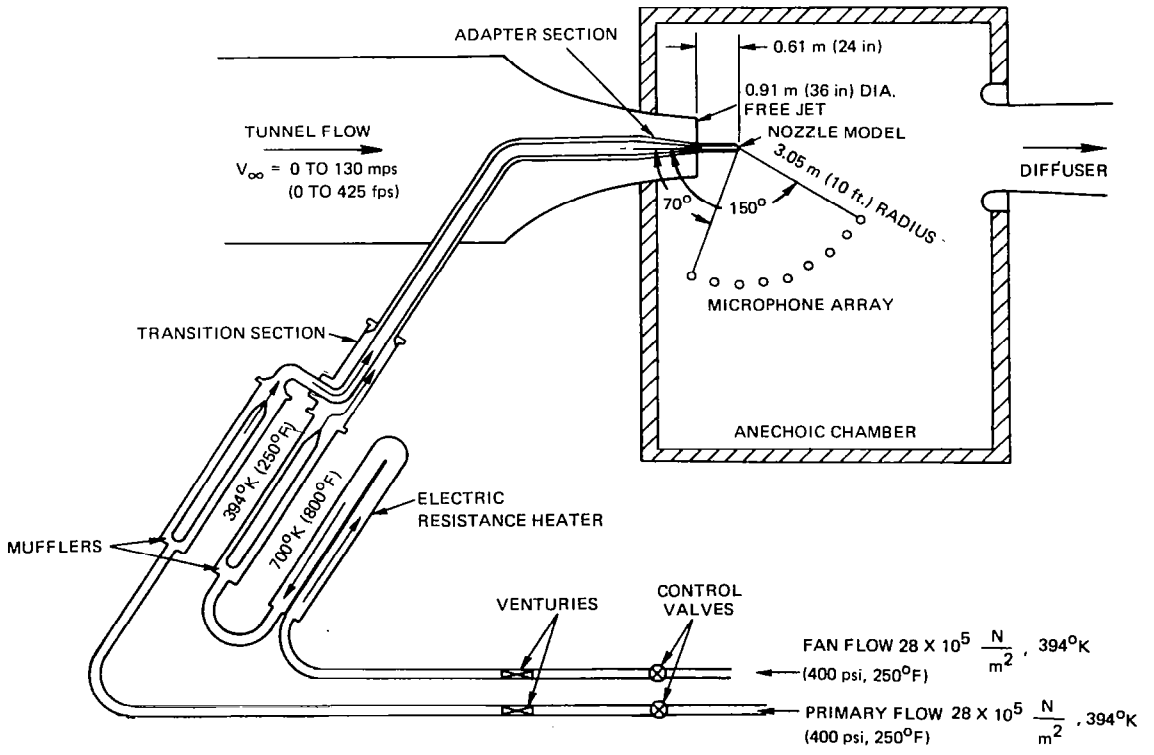

Figure 2 UTRC Acoustic Test Chamber

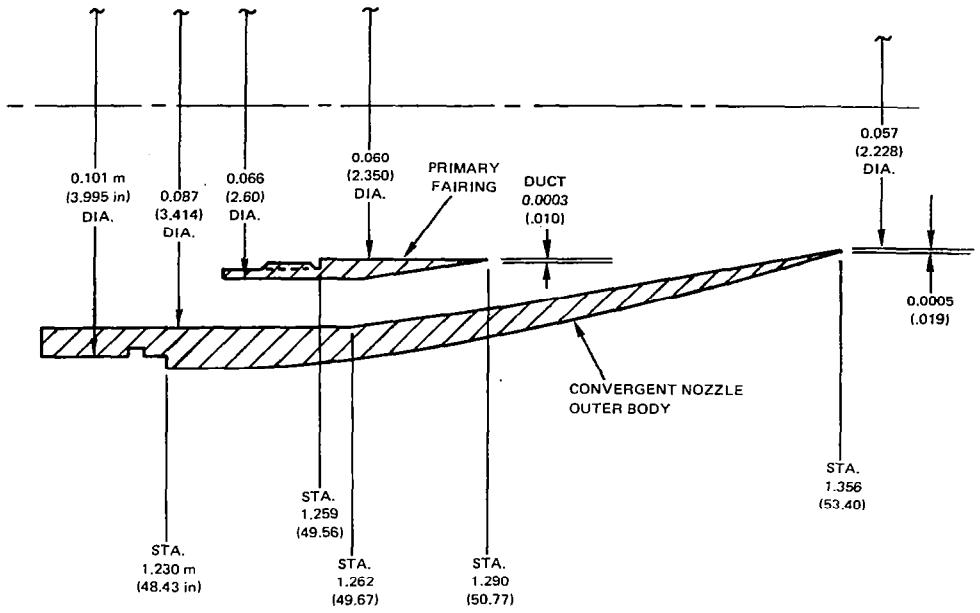

Figure 3 *Reference Convergent Nozzle*

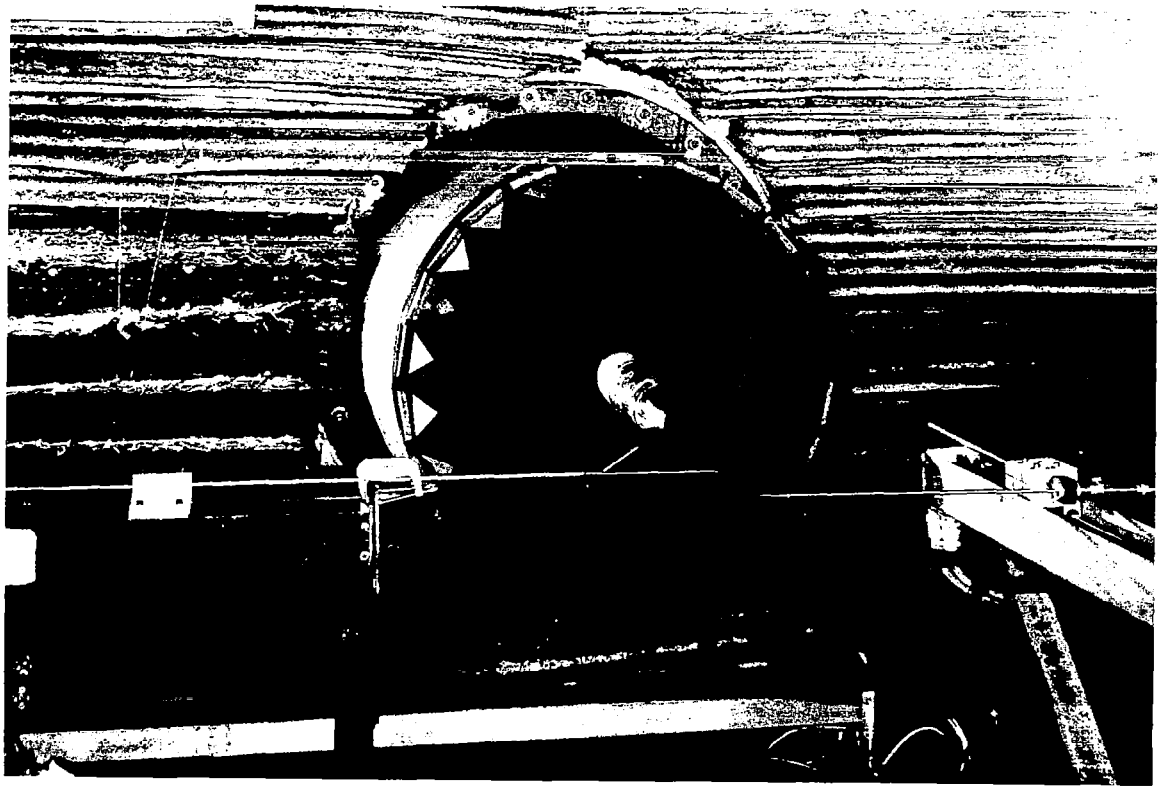

Figure 4 *Hot-Wire Apparatus Deployed with Convergent Nozzle*

The hot wire probe supports were mounted on traverse mechanisms which were bolted to an aluminum plate one-half inch thick. The traverses were aligned so the probes moved orthogonally. The plate was then aligned so that the longitudinal probe traversed parallel to the jet axis.

3.2 DATA ACQUISITION AND REDUCTION

For the mean velocity and turbulence intensity traverses, the data analysis system is shown in Figure 5. The mean and fluctuating linearized anemometer voltage signals (which were proportional to the mean and fluctuating velocities) from probe "A" were read from a digital DC voltmeter (DVM) and RMS AC voltmeter, respectively. A 0.1 Hz low pass filter was used to stabilize the DVM. The calibration curve used to convert voltages to velocities is described in Section 3.4.2. Narrowband frequency spectra were obtained using a Spectral Dynamics 301C Real Time Analyzer, 302C Ensemble Averager, and 305A Octave Analyzer. Figure 6 shows the instrumentation used for spectrum analysis. In calculating a spectrum, data aliasing can occur if the Nyquist frequency (fn) defined as 1/2 h (where 1/h is the data sampling rate) is less than the highest frequency analyzed. The Spectral Dynamics electronics ensured that the Nyquist frequency was three times the highest frequency analyzed, and the Spectral Dynamics Analyzer also contained anti-aliasing filters, which filtered the signal input above the highest frequency analyzed. Therefore, data aliasing did not occur. Cross correlations and autocorrelations were obtained using a Saicor Model SAI-42 Probability and Cross-Properties Analyzer. The arrangement for obtaining cross correlations and autocorrelations is illustrated in Figure 7.

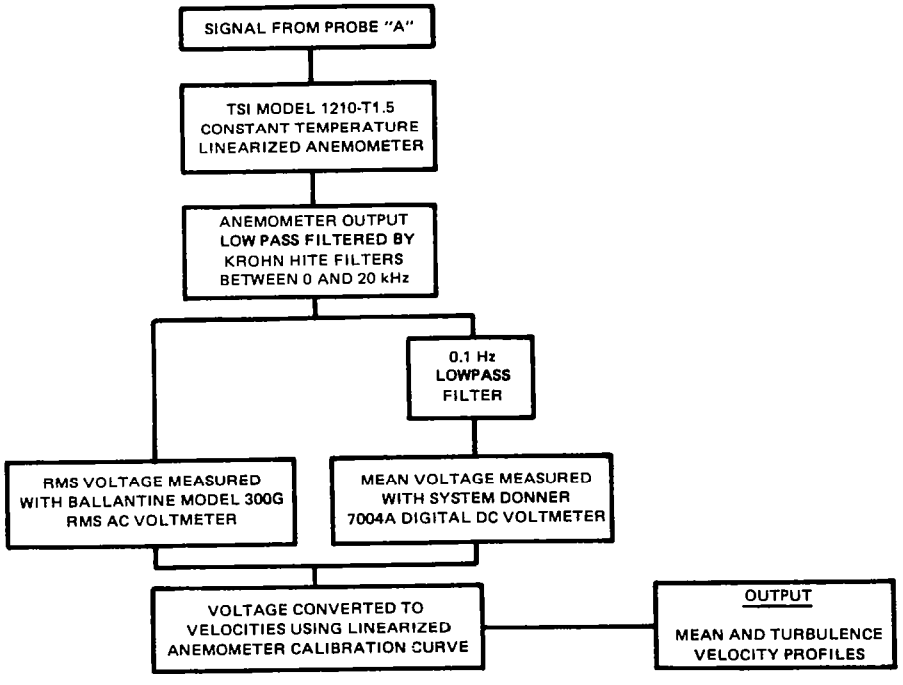

Figure 5 Data Reduction Procedure for Mean and Turbulence Velocity Profiles

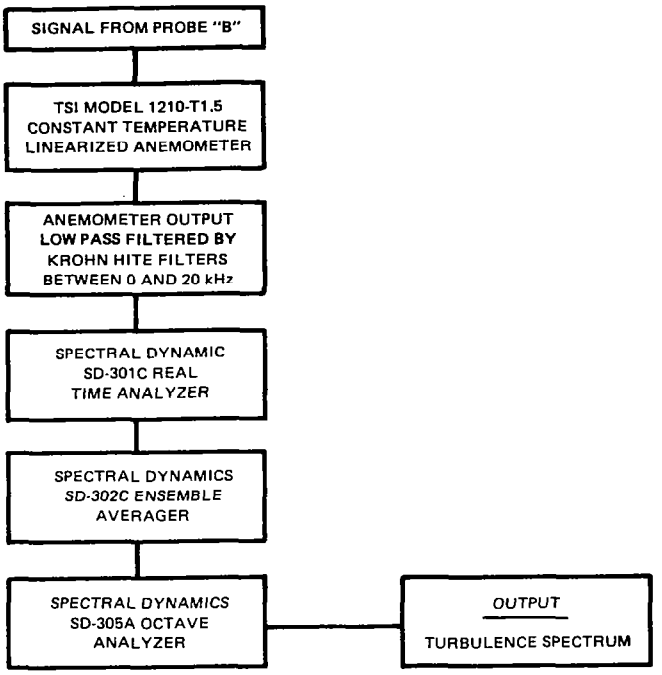

Figure 6 *Data Acquisition Procedure for Turbulence Spectra*

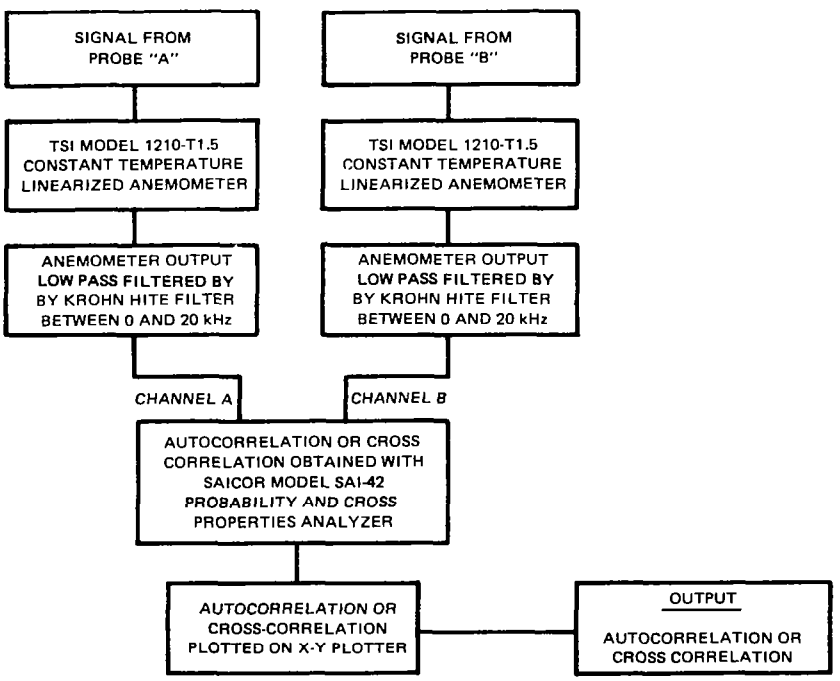

Figure 7 *Data Acquisition Procedure for Cross Correlation and Autocorrelation*

3.3 TEST DEFINITION

3.3.1 Mean Velocity, Turbulence Velocity, and Turbulence Spectra

The test matrix of axial stations as a function of velocity ratio, m, (wind tunnel velocity divided by jet velocity) is shown in Table I. The static measurements (m = 0) were obtained to verify data acquisition procedures by comparison of results with those of Reference 5. For $m \neq 0$, data were taken at x/D = 3 (x is the axial coordinate and D is the jet diameter) to provide data for direct comparison. The other measurement stations were moved downstream with increasing wind tunnel velocity to maintain the same relative position in the shear layer as the jet potential core was lengthened.

TABLE I

TEST MATRIX

Velocity Ratio, m	Axial Station, x/D		
0		3	5
.1	3	5.5	7.7
.3	3	6.8	9.5
.5	3	7.7	12.1

Data obtained at each axial station in Table I were mean velocity and turbulence velocity profiles. Turbulence spectra also were obtained in the peak turbulence region of the shear layer for each axial station. Profiles were obtained by stepping probe "A" across the flow.

3.3.2 Cross Correlation Coefficients and Convection Velocity

For each axial station in Table I, data were obtained at three radial stations to determine normalized cross correlation coefficients and convection velocity. The radial stations were denoted as the inner and outer "edges" of the shear layer and the "center". The "edges" were defined to be the points where the velocity fluctuation level was 50% of the peak level, and the "center" was defined as the peak fluctuation location.

For each radial location, data were obtained at three axial separations. Table II lists the axial separation, defined to be Δx, used for each axial station. The same axial separations were used for all radial stations of a given axial station.

TABLE II

AXIAL SEPARATIONS

Velocity Ratio	$\frac{x}{D}$	Axial Separations $\Delta x/D$
0	3.0	0.27, 1.35, 2.43
0	5.0	0.45, 2.70, 4.95
.1	3.0	0.23, 1.35, 2.48
.1	5.5	0.14, 1.49, 2.84
.1	7.7	0.23, 1.35, 2.48
.3	3.0	0.14, 0.81, 1.49
.3	6.8	0.14, 1.49, 2.84
.3	9.5	0.18, 1.98, 3.78
.5	3.0	0.09, 0.54, 0.99
.5	7.7	0.18, 1.98, 3.78
.5	12.1	0.18, 1.98, 3.78

Data were obtained by holding the upstream probe, probe "A", fixed at one of the radial positions and moving the downstream probe, probe "B", to the appropriate axial separation from Table II. Signals from the two probes were then cross correlated and an autocorrelation for probe B obtained. An autocorrelation for probe "A" was obtained once for each radial position. Filtered cross correlations were obtained at $x/D = 6.8$, $m = 0.3$ for four selected frequency bands (100-250, 250-630, 630-1600, and 1600-4000 Hz).

3.4 TEST PROCEDURE

3.4.1 Determination of Model Nozzle and Wind Tunnel Velocities

The nominal model nozzle exit velocity was maintained at 122 m/sec (400 ft/sec). The pressure ratio required to obtain this velocity was calculated from ideal gas laws using the air temperature. and the total pressure was set based on the pressure ratio and measured test chamber static pressure. When the wind tunnel was operating, the ambient pressure inside the test chamber was reduced, and the nozzle stagnation pressure was adjusted accordingly. Since the wind tunnel flow was driven by a downstream fan, the total pressure for the tunnel was atmospheric, and the flow vanes were adjusted until the ratio of ambient to chamber pressure gave

the pressure ratio required for the desired tunnel velocity. The total pressure for the nozzles was read from a Statham 0–6.895 x 10^5 N/m^2 (0-100 psia) pressure transducer in conjunction with a digital voltmeter, and the chamber static pressure was displayed by a Wallace-Tiernan 0-1.52 m (0–60 in.) of water gauge. The error in nozzle velocity was estimated to be at most 4%, and in the worst case (a wind tunnel velocity of 12.2 m/sec) the estimated error in the wind tunnel velocity was – 10% to +16% (see Appendix A). All the data are reported in the companion comprehensive data report, NASA CR-135238.

3.4.2 Anemometer Calibration

Each probe was calibrated at the beginning of the test day. Since the same operating resistors were used, the probe overheat ratio, and therefore sensitivity, varied with different flow temperatures. Daily calibration minimized the effects that temperature variations would have on the results, and spot checks were made where possible to insure that probe sensitivity did not change appreciably with the minor temperature changes that occurred during a run. Figure 8 illustrates a typical probe calibration curve. Calibration curves were used to convert the mean and RMS voltage outputs (see Figure 5) into mean velocity and RMS turbulence levels.

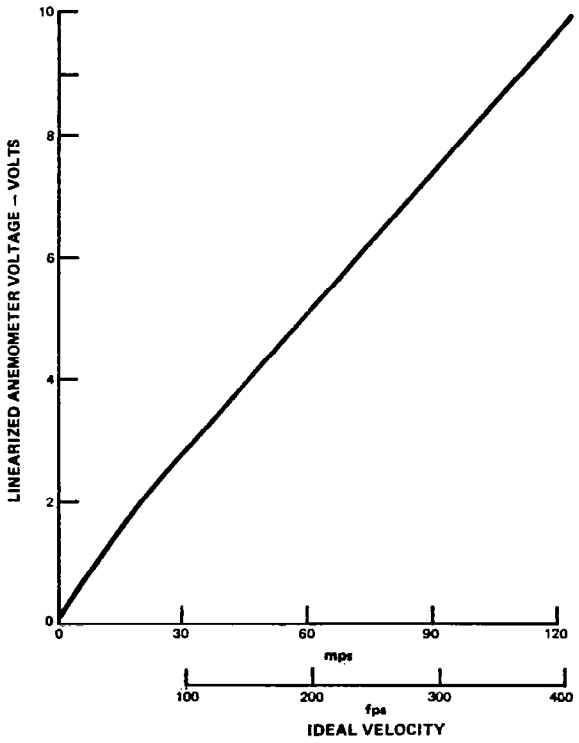

Figure 8 Linearized Anemometer Calibration Curve

The anemometer frequency response was also checked using the internal 1 kHz square wave generator. The typical anemometer response to the square wave input is shown in Figure 9. With a time constant, τ, defined as shown, the frequency response calculated from

$$f = \frac{1}{1.5\tau} ,$$

was always in excess of 80 kHz. In some instances the anemometer controls were adjusted to this fairly low value so that the high frequency resonance observed at 200 to 500 kHz was reduced. However, the useful frequency range extended well above the region of interest of 20 kHz.

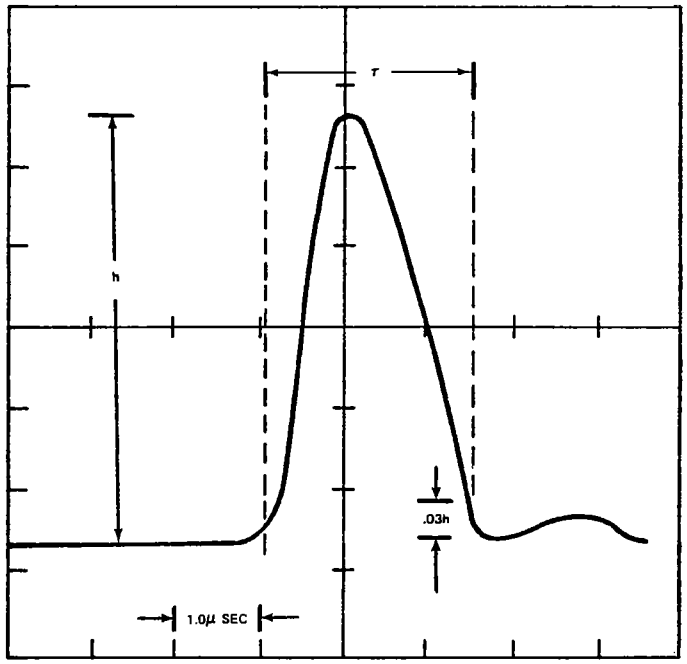

Figure 9 *Hot-Wire Anemometer Frequency Response*

4.0 RESULTS AND DISCUSSION

4.1 MEAN VELOCITY

The mean velocity was normalized by the relation

$$\hat{U} = \frac{U - U_e}{U_j - U_e}, \tag{1}$$

where U is the measured velocity, U_j is the jet velocity, U_e is the external flow velocity, and $\hat{U}$ the normalized velocity. The normalized velocity profiles from different axial stations or velocity ratios, m, were collapsed by plotting $\hat{U}$ versus the similarity parameter

$$\hat{r} = \frac{r - r_{0.5}}{b}, \tag{2}$$

where r is the radial co-ordinate, b is the shear layer thickness, and $r_{0.5}$ is the radial position where $\hat{U} = 0.5$. The shear layer thickness b is defined as

$$b = r_{0.95} - r_{0.05},$$

where $r_{0.95}$ and $r_{0.05}$ are the radial positions where $\hat{U} = 0.95$ and 0.05, respectively. In Figure 10, $\hat{U}$ is plotted versus $\hat{r}$ at the axial station x/D = 3 and velocity ratios m of 0, .1, .3, and .5. Also shown is the curve from Reference 5 obtained for a static jet. Agreement is good between the normalized velocities in this report and those from Reference 5. Figure 11 contains plots of the normalized velocity profiles for fixed velocity ratio but different axial stations. The data collapse in Figures 10 and 11 show that equations (1) and (2) completely normalize the effects of relative velocity and axial position. Agreement of the normalized profiles with data for a static jet from Reference 5 is good.

4.2 MIXING LAYER GROWTH

The mixing layer width was found to grow linearly with downstream distance. The effect of external velocity on mixing layer width is shown in Figure 12. The data collapse, using a least squares fit, to the line

$$\frac{\sqrt{1+m}}{1-m}\,\frac{b}{D} = 0.24 + 0.13\,\frac{x}{D}. \tag{3}$$

At a fixed axial station, the mixing layer width was reduced as velocity ratio was increased by the factor $(1 - m)/\sqrt{1+m}$.

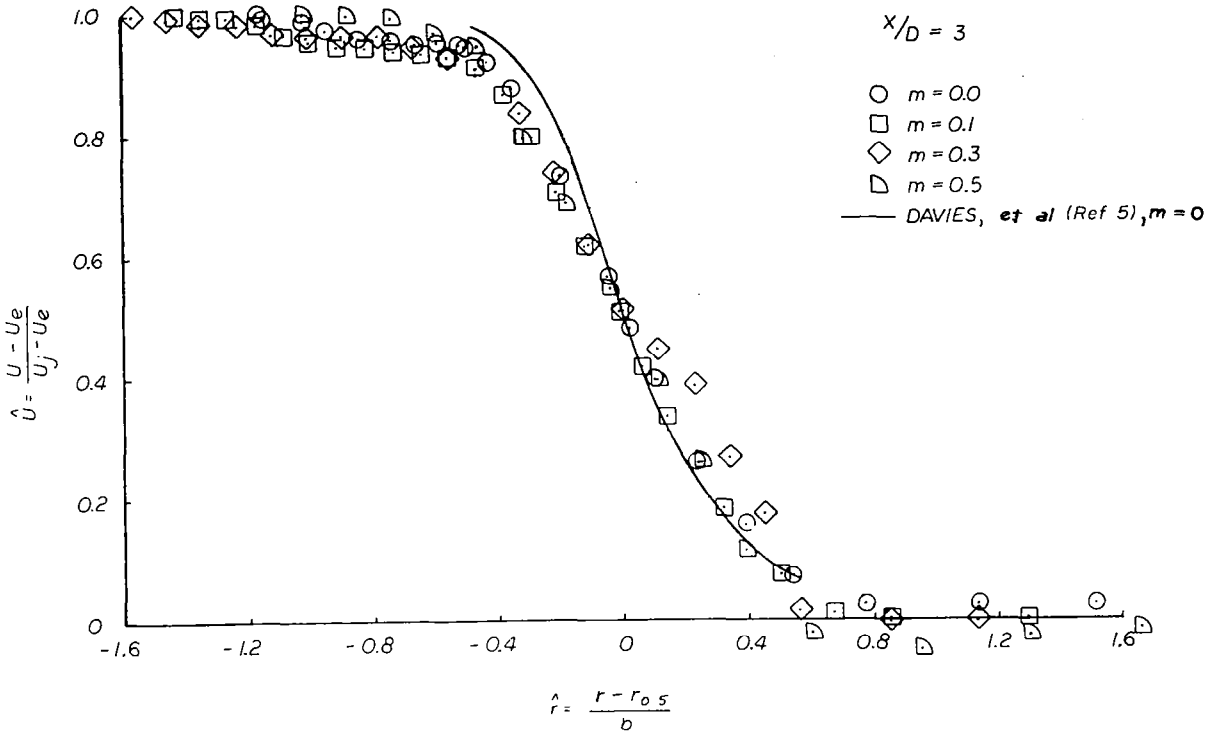

Figure 10 Mean Velocity Normalization with Respect to Velocity Ratio at a Constant Axial Location

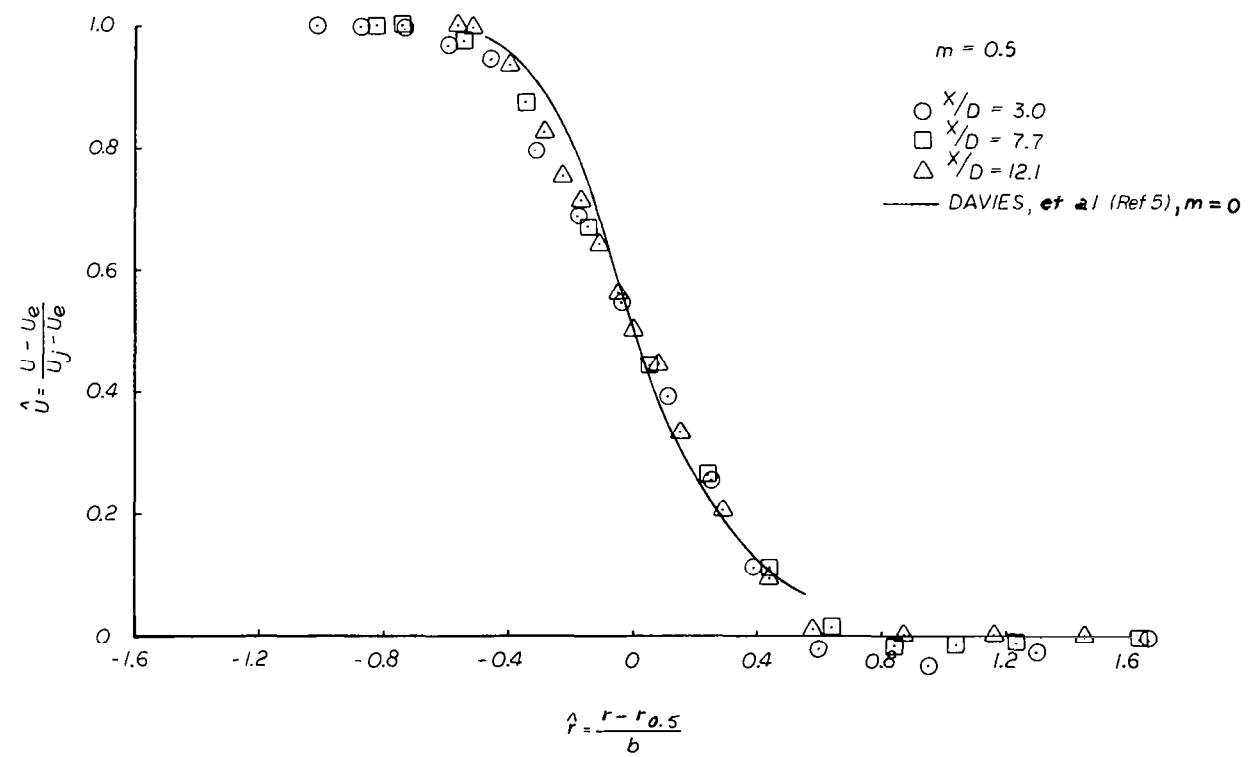

Figure 11 Mean Velocity Normalization with Respect to Axial Location at Constant Velocity Ratio

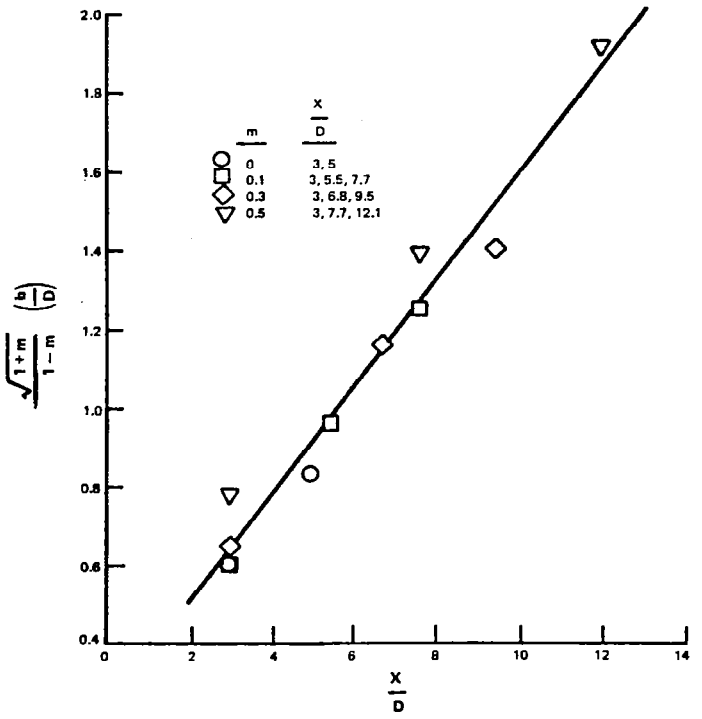

Figure 12 Mixing Layer Growth Normalized with Respect to Velocity Ratio

4.3 TURBULENCE MEASUREMENTS

4.3.1 Turbulence Spectra

Turbulence spectra were obtained in the peak turbulence region of the shear layer as described in Sections 3.2 and 3.3. Figure 13 contains plots of turbulence spectra at the axial station x/D = 3.0 and for velocity ratios of 0, .3, and .5. The low frequency content of the spectra decreased as m increased, but the levels at high frequencies remained constant. This suggests that flight effects did not change the turbulence microscale associated with the high frequency levels but did affect the large scale eddies associated with the low frequency levels.

A line representing the – 5/3 power law also is shown in Figure 13. While the data are close to this law, the slope actually is found to be – 2.04. This is in very good agreement with the results of previous experiments, that show values of –2.07, –2.08, –2.09 (References 4, 7, and 11, respectively).

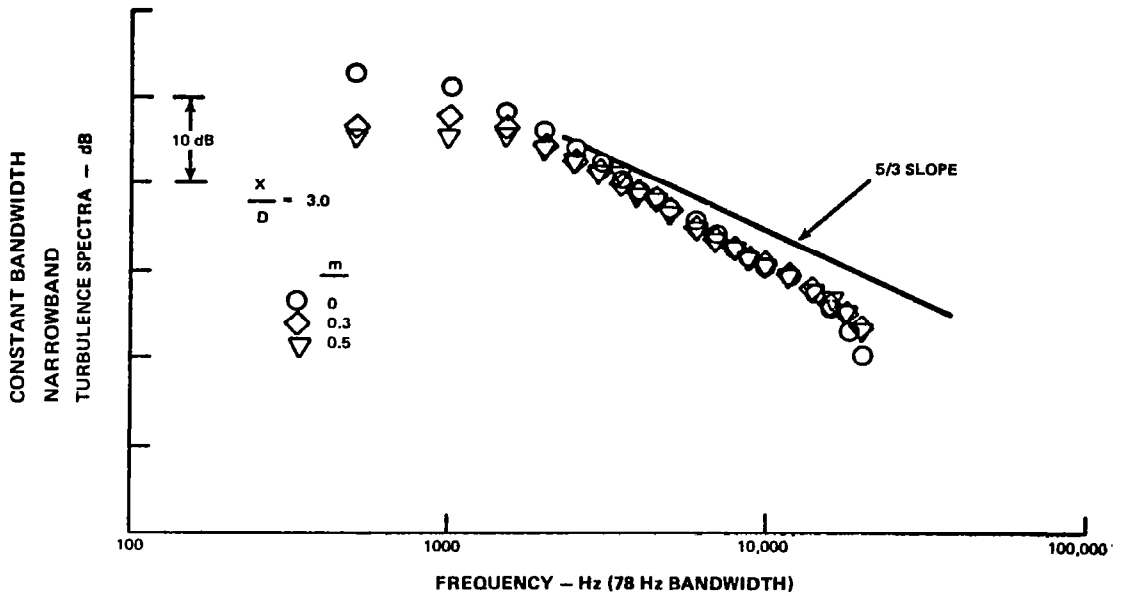

Figure 13 *Turbulence Spectra in the Peak Turbulence Region of the Shear Layer at Constant Axial Location*

4.3.2 Turbulence Intensity

The turbulence profiles obtained for a velocity ratio of zero are shown for axial stations (x/D) of 3 and 5 in Figure 14. The maximum level measured was on the order of 10% as compared to a level of 13% measured at a similar axial location and jet Mach number in Reference 4. The slightly lower turbulence levels were caused by the addition of a small amount of clay at the base of the probe holder to remove a probe vibration which generated spurious signals near 10 kHz. This forced the flow through a small contraction thus reducing the turbulence level. This reduction did not affect mean flow cross correlation or turbulence spectrum measurements. All turbulence and mean flow measurements, except for the turbulence intensity, obtained under static conditions agreed with those obtained in References 4, 7 and 11. As discussed in Section 4.3.1, turbulence spectra obtained in this investigation agreed with those obtained in References 4, 5, 7 and 11.

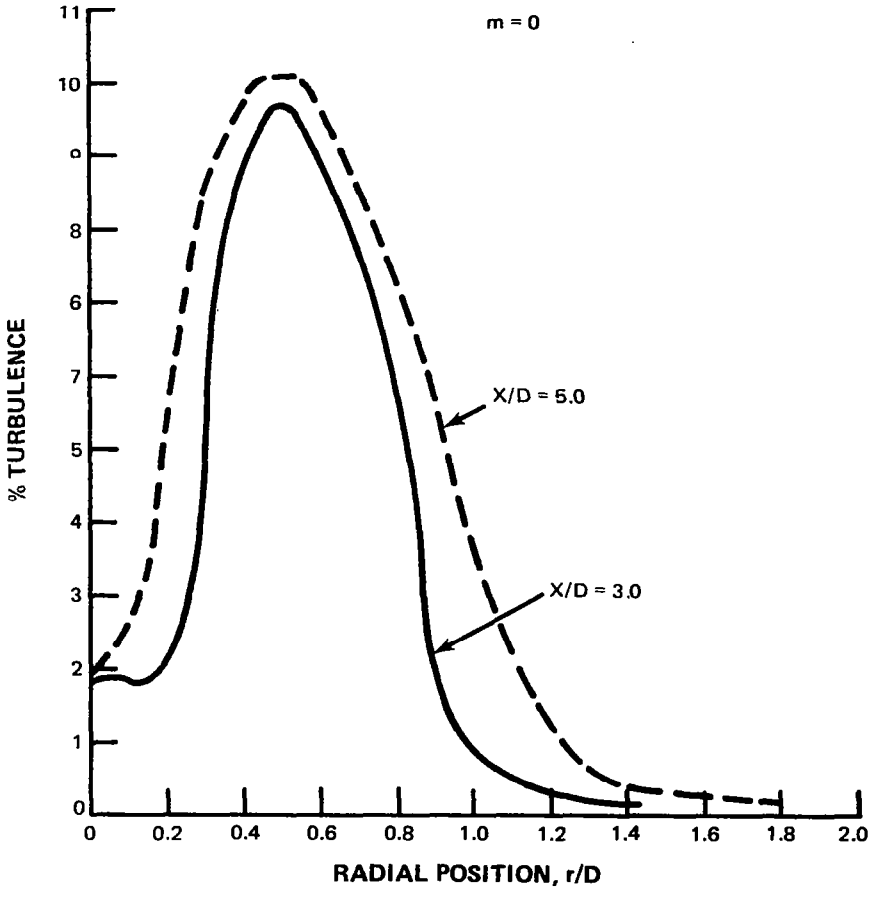

Figure 14 Turbulence Intensity Profiles at Static Conditions

Peak turbulence intensity at an axial station of x/D = 3.0 was found to decrease with increasing external velocity as shown in Figure 15. The reduction is represented by the line,

$$\frac{u_p'}{u_p'\,m = 0} = (1 - m)^{0.7}, \qquad (4)$$

where u_p' is the peak fluctuating velocity component at a given x/D. The exponent 0.7 was also determined in Reference 10 for several velocity ratios and axial stations.

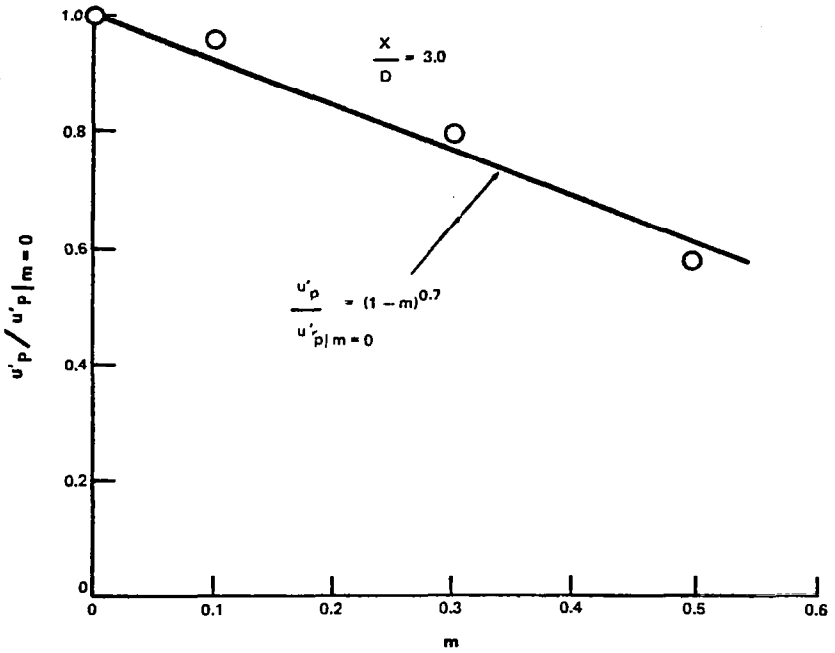

Figure 15 Effect of Velocity Ratio on Peak Turbulence Level at Constant Axial Location

4.4 TURBULENCE CONVECTION VELOCITY

The convection velocity was determined by cross correlating the fluctuating signals of two hot-wires which were axially separated by a distance Δx. This distance was divided by the time delay (τ_{max}) for the maximum cross correlation coefficient to give the local convection velocity U_c; that is,

$$U_c = \frac{\Delta x}{\tau_{max}} .$$

The values of probe separation used to calculate convection velocities were shown in Table II in Section 3.2. A sample calculation of the convection velocity and a table of all calculated convection velocities are contained in Appendix B. Initially it was found that the smallest probe separations resulted in unreliable calculated convection velocities, probably due to probe interference. This increment was made larger in succeeding tests, but only a few of the small axial separations provided valid results. However, the two larger separations provided values of convection velocity which differed by less than 10%, indicating that a valid measure of the convection velocity had been obtained.

The convection velocity was normalized by the relation

$$\hat{U}_c = \frac{U_c - U_e}{U_j - U_e} . \qquad (4)$$

The normalized convection velocity in the peak turbulence region of the shear layer was plotted in Figure 16 to determine if $\hat{U}_c$ is independent of velocity ratio and axial position. The overall data collapse indicates that $\hat{U}_c$ is a constant, 0.57.

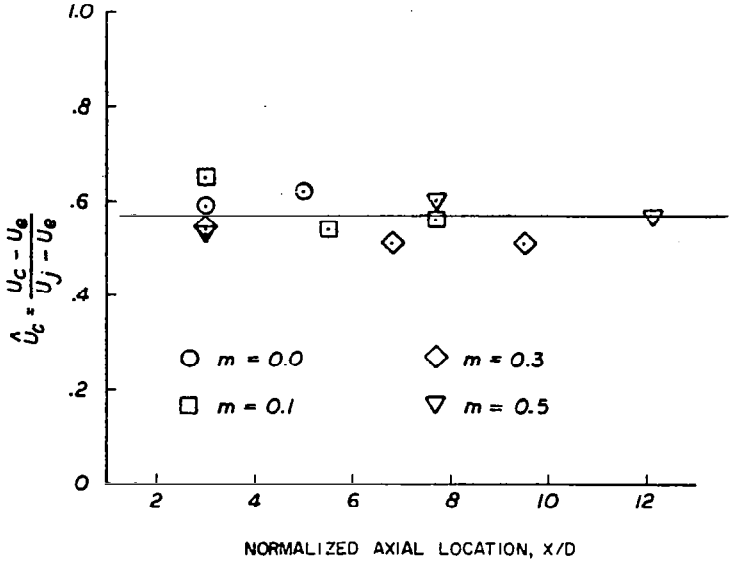

Figure 16 Normalized Convection Velocity in the Peak Turbulence Region of the Shear Layer

Figure 17 contains a plot of $\hat{U}_c$ versus a normalized parameter

$$\tilde{r} = \frac{r - r_p}{b} , \qquad (5)$$

where r is the radial coordinate, and r_p is the peak turbulence radial coordinate. The normalized convection velocity decreases from a maximum value of 0.85 at the inner edge of the shear layer to about 0.45 at the outer edge of the shear layer. The general data collapse indicates that convection velocity can be normalized by the expressions in Equations (4) and (5). The normalization removes the effect of velocity ratio and axial position.

Convection velocity was determined as a function of frequency at x/D = 6.8, m = 0.3. The normalized convection velocity is plotted as a function of frequency in Figure 18. The high frequency turbulence components have a larger convection velocity than the low frequency components. The unfiltered convection velocity is a weighted average of the velocities of the different frequencies. Comparison of the unfiltered convection velocity with the filtered convection velocities shows that the velocity of the peak frequency of the turbulence spectrum (600-1000 Hz) is approximately the same as the unfiltered convection velocity.

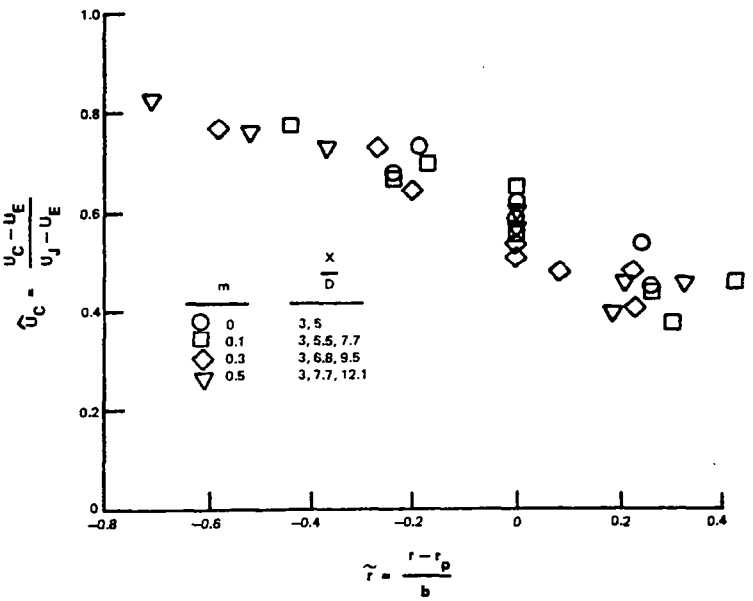

Figure 17 *Radial Variation of Convection Velocity Normalized with Respect to Velocity Ratio and Axial Location*

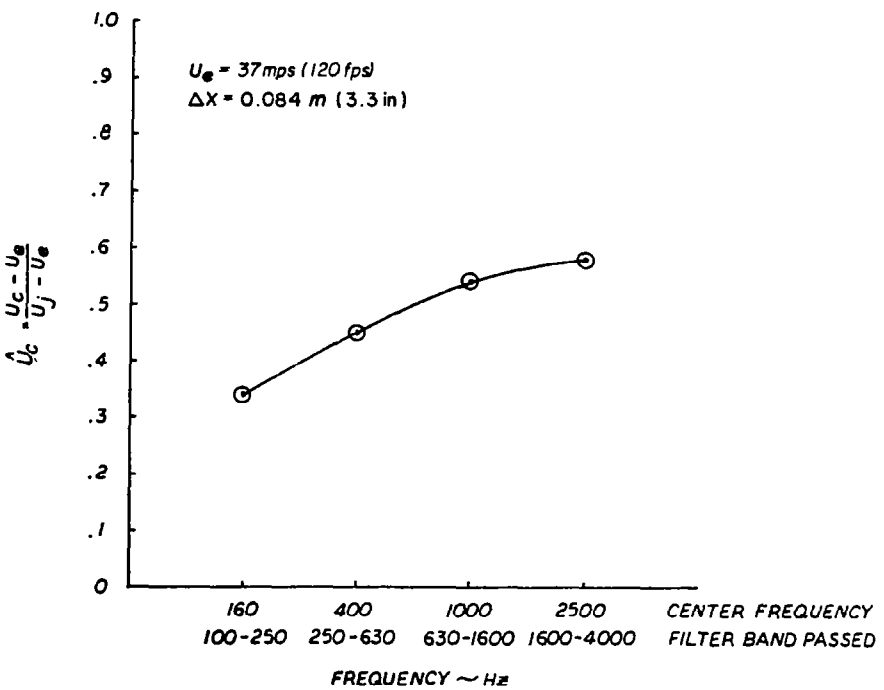

Figure 18 *Variation of Filtered Normalized Convection Velocity with Frequency*

5.0 CONCLUSIONS

The following conclusions are the major results of this investigation:

- Mean velocity profiles may be normalized with respect to axial position and relative velocity.

- The mixing layer width grows linearly with axial distance and is reduced in width with relative velocity, at fixed axial position, by the ratio $(1\text{-}m)/\sqrt{1+m}$.

- Turbulence spectra show that only the low frequency levels associated with large scale eddies are reduced with forward velocity while the high frequency levels associated with the turbulence microscale remain unchanged.

- Turbulence intensity is dominated by the low frequency behavior of the turbulence spectrum and is reduced with relative velocity by the function $(1\text{-}m)^{0.7}$.

- Convection velocity may be normalized with respect to axial position and velocity ratio across the entire jet shear layer.

- The unfiltered normalized convection velocity is a constant, 0.57, in the peak turbulence region of the shear layer.

- The high frequency, microscale turbulence components have a significantly larger convection velocity than the low frequency components.

- The turbulence convection velocity measured for the overall unfiltered signal was similar to that measured for the peak frequency band of the turbulence spectrum that contained the bulk of the energy.

APPENDIX A

ESTIMATE OF ERRORS

An important consideration in the measurement system is the degree of accuracy to which the flow conditions can be set. The nozzle total pressure was set to give a jet velocity of 122 m/sec (400 ft/sec) based on ideal gas relationships and the measured jet total temperature. The variation in jet velocity then depends on the total pressure instrumentation and variation of total temperature with time. The total pressure instrumentation was calibrated at atmospheric pressure and at 6.895×10^5 N/m^2 (100 psia), which were provided by a barometer and Wallace-Tiernan 0 - 6.895×10^5 N/m^2 (0 – 100 psia) pressure gauge, respectively. A voltage signal proportional to pressure was provided by a Statham transducer and presented to two places on a digital voltmeter. For a nozzle pressure ratio of 1.1 (approximately equal to that required for 122 m/sec (400 ft/sec), the total pressure was approximately 1.11×10^5 N/m^2 (16.17 psia). Errors in setting this pressure would therefore be due mainly to three sources: changes in nozzle stagnation temperature, drift of the nozzle operating condition with time, and drift of the electronic pressure display. The latter conditions of drift were monitored constantly and were maintained to less than 6.895×10^2 N/m^2 (0.1 psia). An error as large as 6.895×10^2 N/m^2 (0.1 psia) in the atmospheric reference would cause an error in pressure ratio of less than 0.1%.

The possible error due to drift of the nozzle operating condition is on the order of 1.379×10^3 N/m^2 (0.2 psia), which is approximately 0.2% error in pressure ratio. In the vicinity of 122 m/sec (400 ft/sec), this would become a velocity error of approximately 3.05 m/sec (10 ft/sec) or 2.5%.

Changes in nozzle stagnation temperature also have an effect on nozzle velocity. During a run the maximum observed temperature change was 2.8°K (5°F). Also, in some instances the fan and primary temperatures were found to differ by 4.44°K (8°F). At the average of operating conditions, these errors would result in a total velocity error of about 1.22 to 1.52 m/sec (4 to 5 ft/sec), or 1%.

The total error in setting the nozzle operating condition would then be less than 4.57 m/sec (15 ft/sec), or about 4%.

A similar analysis may be carried out for the tunnel flow velocity. The Wallace-Tieman gauge displayed the difference between the static pressure in the test chamber and the atmosphere in inches of water; 0.005/m (0.2 in.) was the smallest division. With the maximum gauge error being 0.0025 m (0.1 in.) of water, the following variations will occur in the nozzle exit velocity for an assumed total temperature of 283°K (50°F). At 283°K (50°F), 122 m/sec (40 ft/sec) will be obtained if the pressure ratio is 1.000916, resulting in a gauge reading of 0.0094 m (0.37 in.) H_2O. A setting of 0.0076 m (0.3 in.) results in a flow velocity of 11.0 m/sec (36 ft/sec) while 0.013 m (0.5 in.) gives a velocity of 14.0 m (46 ft/sec), an error range of −10% to +16%. The error range for the higher velocities may be similarly calculated. At a nominal tunnel velocity of 36.6 m/sec (120 ft/sec), the error range is from −2.1 to +1.2%, 0.081 m to 0.086 m (3.2 in. to 3.4 in) of H_2O, while at 61.0 m/sec (200 ft/sec) the range is from −.7 to +.4%, 0.23 m to 0.24 m (9.1 in. to 9.3 in.) of H_2O. At the higher velocities, the errors in setting the flow velocity may be neglected.

APPENDIX B

TABULATION OF CONVECTION VELOCITIES

The convection velocity is determined by cross correlating the fluctuating signals of two hot wires which are separated axially by a distance ΔX. Convection velocities are calculated by dividing the separation ΔX by the time delay for the maximum cross correlation coefficient.

A sample convection velocity may be calculated as follows:

for m = o, x/D = 3.0 and R/D = 0.363

$\Delta X = 0.6$ in.
$\tau_{max} = 2.5 \times 10^{-4}$ sec.

The convection velocity U_C, is

$$U_C = \frac{0.6}{(12)(2.5 \times 10^{-4})} = 200 \text{ ft/sec}$$

A tabulation of all the calculated convection velocities is presented below.

CONVECTION VELOCITY

$m=u_e/u_j$	$\frac{X}{D}$	$\frac{R}{D}$	ΔX (in)	u_c (fps)	$m=u_e/u_j$	$\frac{X}{D}$	$\frac{R}{D}$	ΔX (in)	u_c (fps)
0	3.0	0.363	0.6	200	0.1	7.7	-0.006	0.5	306
		0.363	3.0	281			-0.006	3.0	301
		0.363	5.4	282			-0.006	5.5	337
		0.507	0.6	213			0.462	0.5	177
		0.507	3.0	230			0.462	3.0	238
		0.507	5.4	254			0.462	5.5	239
		0.665	0.6	106			0.782	0.5	123
		0.665	3.0	181			0.782	3.0	160
		0.665	5.4	190			0.782	5.5	189
	5.0	0.304	1.0	278	0.3	3.0	0.410	0.3	240
		0.304	6.0	297			0.410	1.8	319
		0.304	11.0	278			0.410	3.3	299
		0.462	1.0	220			0.518	0.3	216
		0.462	6.0	250			0.518	1.8	259
		0.462	11.0	237			0.518	3.3	263
		0.665	1.0	167			0.608	0.3	174
		0.665	6.0	217			0.608	1.8	246
		0.665	11.0	207			0.608	3.3	246
0.1	3.0	0.381	0.5	278		6.8	0.352	0.3	219
		0.381	3.0	278			0.352	3.3	299
		0.381	5.5	296			0.352	6.3	309
		0.471	0.5	189			0.496	0.3	179
		0.471	3.0	263			0.496	3.3	262
		0.471	5.5	270			0.496	6.3	269
		0.687	0.5	194			0.658	0.3	132
		0.687	3.0	199			0.658	3.3	237
		0.687	5.5	202			0.658	6.3	236
	5.5	0.290	0.3	196		9.5	-0.045	0.4	347
		0.290	3.3	289			-0.045	4.4	327
		0.290	6.3	282			-0.045	8.4	318
		0.484	0.3	147			0.450	0.4	185
		0.484	3.3	239			0.450	4.4	256
		0.484	6.3	239			0.450	8.4	252
		0.700	0.3	86			0.518	0.4	139
		0.700	3.3	198			0.518	4.4	255
		0.700	6.3	202			0.518	8.4	238

$m=u_e/u_j$	$\frac{X}{D}$	$\frac{R}{D}$	ΔX (in)	u_c (fps)
0.5	3.0	0.401	0.2	333
		0.401	1.2	333
		0.401	2.2	340
		0.518	0.2	269
		0.518	1.2	286
		0.518	2.2	306
		0.586	0.2	157
		0.586	1.2	286
		0.586	2.4	276
	7.7	-0.101	0.4	980
		-0.101	4.4	367
		-0.101	8.4	375
		0.304	0.4	292
		0.304	4.4	324
		0.304	8.4	328
		0.489	0.4	256
		0.489	4.4	302
		0.489	8.4	295
	12.1	-0.118	0.4	483
		-0.118	4.4	353
		-0.118	8.4	350
		0.287	0.4	298
		0.287	4.4	319
		0.287	8.4	306
		0.431	0.4	300
		0.431	4.4	286
		0.431	8.4	269

R/D = 0.496

$m = u_e/u_j$	$\frac{X}{D}$	ΔX (in)	Filtered Frequency (kHz)	u_c (fps)
0.3	6.8	3.3	0.1 – 0.25	217
			0.25 – 0.63	250
			0.63 – 1.60	275
			1.60 – 4.00	285

LIST OF SYMBOLS

b	Mixing layer width
D	Diameter of convergent nozzle
f	Frequency response of the hot wire anemometer
m	Velocity ratio of the wind tunnel velocity divided by the jet velocity
r	Radial distance measured from the jet centerline
$r_{0.5}$	Radial distance at which $\hat{U} = 0.5$
$r_{0.05}$	Radial distance at which $\hat{U} = 0.05$
$r_{0.95}$	Radial distance at which $\hat{U} = 0.95$
$\hat{r}$	Normalized radial co-ordinate, $\hat{r} = (r - r_{0.5})/b$, for mean velocity
$\tilde{r}$	Normalized radial co-ordinate, $\tilde{r} = (r - r_p)/b$, for convection velocity
r_p	Radial distance at which the peak turbulence was obtained
u_p'	Peak RMS turbulence
$u'_{p\|m=0}$	Peak RMS turbulence obtained under static conditions
U	Measured mean velocity
$\hat{U}$	Normalized mean velocity defined by $\hat{U} = (U - U_e)/U_j - U_e)$
U_e	External flow velocity of free jet wind tunnel calculated from ideal gas laws
U_j	Jet velocity calcualted from ideal gas laws
U_c	Turbulence convection velocity
$\hat{U}_c$	Normalized turbulence convection velocity defined by $\hat{U}_c = (U_c - U_e)/(U_j - U_e)$
x	Axial distance measured from nozzle exit plane
Δx	Separation between probes A and B defined by $\Delta x = x_B - x_A$
x_A	Axial location of probe "A"
x_B	Axial location of probe "B"
τ	Time constant for anemometer electronics
τ_{max}	Time delay for the maximum cross correlation coefficient for a given separation of probes "A" and "B"

REFERENCES

1. Packman, A. B., K. W. Ng and R. W. Paterson, "Effect of Simulated Forward Flight on Subsonic Jet Noise", Journal of Aircraft, December , 1976.

2. Cocking, B. J. and W. D. Bryce, "Subsonic Jet Noise in Flight Based on Some Recent Wind-Tunnel Results", AIAA Paper No. 75-462 (1975).

3. Bushell, K. W., "Measurement and Prediction of Jet Noise in Flight", AIAA Paper 75-461 (1975).

4. Laurence, James, "Intensity, Scale, and Spectra of Turbulence in Mixing Region of a Free Subsonic Jet", NACA Report 1292 (1956).

5. Davies, P. O. A. L., M. J. Fisher and M. J. Barratt, "The Characteristics of the Turbulence in the Mixing Region of a Round Jet", JFM 15, pp 337-367 (1963).

6. Nayer, B. M., T. E. Siddon, and W. T. Chu, "Properties of the Turbulence in the Transition Region of a Round Jet", UTIAS Technical Note No. 131, (1969).

7. Spencer, B. W. and B. G. Jones, "Statistical Investigation of Pressure and Velocity Fields in the Turbulent Two-Stream Mixing Layer", AIAA Paper 71-613 (1971).

8. Jones, B. G., H. P. Planchon and R. J. Hammersley, "Turbulent Space-Time Correlation Measurements in a Plane Two-Stream Mixing Layer at Velocity Ratio 0.3 ", AIAA Paper 73-225 (1973).

9. Wygnanski, I. and H. E. Fiedler, "The Two Dimensional Mixing Region", JFM 41, pp. 327-361 (1970).

10. Plumblee, H. E. ed., "Effects of Forward Flight on Turbulent Jet Mixing Noise." NASA CR-2702, July 1976.

11. de Belleval, J., F. O. Leuchter, and M. Perulli, "Simulation of Flight Effects on the Structure of Jet Mixing Layers for Acoustic Applications," AIAA Paper No. 76-559 (1976).

12. Larson, R. S., C. J. McColgan and A. B. Packman, "Jet Noise Source Modification Due to Forward Flight", AIAA Paper 77-58.

13. Paterson, R. W., P. G. Vogt and W. M. Foley, "Design and Development of the United Aircraft Research Laboratories Acoustic Research Tunnel", J. Aircraft, 10;7, p. 427, July (1973).

1. Report No.	2. Government Accession No.	3. Recipient's Catalog No.
NASA CR-2949		

4. Title and Subtitle	5. Report Date
MEAN VELOCITY, TURBULENCE INTENSITY AND TURBULENCE CONVECTION VELOCITY MEASUREMENTS FOR A CONVERGENT NOZZLE IN A FREE JET WIND TUNNEL	April 1978
	6. Performing Organization Code
7. Author(s)	8. Performing Organization Report No.
C. J. McColgan and R. S. Larson	PWA-5506
	10. Work Unit No.
9. Performing Organization Name and Address	
Pratt & Whitney Aircraft Group United Technologies Corporation East Hartford, Connecticut 06108	11. Contract or Grant No. NAS3-17866
	13. Type of Report and Period Covered
12. Sponsoring Agency Name and Address	Contractor Report
National Aeronautics and Space Administration Washington, D.C. 20546	14. Sponsoring Agency Code

15. Supplementary Notes

Final report. Project Manager, Orlando A. Gutierrez, V/STOL and Noise Division, NASA Lewis Research Center, Cleveland, Ohio 44135.

16. Abstract

The effect of flight on the mean flow and turbulence properties of a 0.056 m circular jet were determined in a free jet wind tunnel. The nozzle exit velocity was 122 m/sec, and the wind tunnel velocity was set at 0, 12, 37, and 61 m/sec. Measurements of flow properties including mean velocity, turbulence intensity and spectra, and eddy convection velocity were carried out using two linearized hot wire anemometers. These data are all presented in the companion Comprehensive Data Report NASA CR-135238. Normalization factors were determined for the mean velocity and turbulence convection velocity.

17. Key Words (Suggested by Author(s))	18. Distribution Statement
Turbulence measurements Free jet wind tunnel Hot wirea nemometers Eddy convection velocity	Unclassified - unlimited STAR Category 02

19. Security Classif. (of this report)	20. Security Classif. (of this page)	21. No. of Pages	22. Price*
Unclassified	Unclassified	28	A03

* For sale by the National Technical Information Service, Springfield, Virginia 22161

NASA-Langley, 1978